Journal of Radioanalytical and Nuclear Chemistry (2021) 330:1397–1408
https://doi.org/10.1007/s10967-021-07965-9

# Luminescence and dosimetric characteristics of microcrystalline $SrB_4O_7:Eu^{3+}$ synthesized by solid state diffusion method

Neyaz Ali[1] · P. D. Sahare[1] · Avinash R. Kachere[2] · Prashant M. Kakade[2] · Nandkumar T. Mandlik[2] · S. D. Dhole[3]

Received: 29 April 2021 / Accepted: 19 August 2021 / Published online: 13 October 2021
© Akadémiai Kiadó, Budapest, Hungary 2021

## Abstract

Microcrystalline $SrB_4O_7:Eu^{3+}$ (SBO) synthesized using strontium carbonate, boric acid and europium chloride as precursors by solid state diffusion method with different concentrations of europium. The microcrystalline powder samples were annealed and quenched at different temperatures in the range of 400–900 °C for 2 h in air and were characterized by XRD, SEM, EDS techniques. The phosphor material with 0.2 mol% europium doping and annealed at 700 °C shows maximum TL intensity and PL studies show presence of Eu in 2 + and 3 + ionic states. The dosimetry characteristics show that the phosphor could be used for high dose measurements.

**Keywords** $SrB_4O_7:Eu^{3+}$ TLD phosphor · Solid state diffusion method · Thermoluminescence (TL) · Photoluminescence (PL) · Dosimetry characteristics · Trapping parameters

## Introduction

Thermoluminescence (TL) is a familiar technique, used for various applications in radiation dosimetry. The materials activated with certain impurities (popularly known as phosphors) when irradiated with high-energy (ionizing radiations) produce electron traps and holes (luminescence centers). They are mostly stable at room temperature but emit visible light during their recombinations on stimulating optically or simply by heating. The intensity of luminescence thus produced by thermal stimulation (TL) has generally linear relationship (in a specific dose range) with the ionizing radiation dose(s) (absorbed doses) given to the phosphor material and unknown absorbed dose(s) could thus be estimated by calibration. In other words, some little amount of energy is stored in the material in the form of defects which gets released on stimulation in the form of visible light, converted into electrical signal and used for estimating/monitoring high-energy radiation doses. This is necessary as high-energy radiations are hazardous to living beings. TL has expanded its applications in personnel, clinical and environmental dosimetry, medical dosimetry, space dosimetry, archaeological and geological dating, etc. [1–4]. Luminescence of rare earth ions activated alkaline earth borates has been well studied by several workers as found in the literature [5–14], particularly strontium tetraborate ($SrB_4O_7$, here represented as SBO) because of its special structure [15]. The crystal structure of SBO is orthorhombic with space group $Pnm2_1(31)$. The structure of SBO contain a rigid 3-dimentisonal $B_4O_7$ network of which each corner attached to $BO_4$ tetrahedrons, with the strontium atoms positioned in the larger confinement of atomic structure by nine oxygen atoms [16, 17]. These confinements of oxygen are large enough to house the activator ions (rare earth ions such as, $Eu^{2+}$, $Eu^{3+}$, $Dy^{2+}$, $Sm^{2+}$, etc.) without breaking the borate networks, hence targeted for various applications. Strontium tetraborate is unique compound which devises excellent nonlinear optical properties with high mechanical strength, nonhygroscopic in nature and high optical damage threshold [18].

Rare-earth and non-rare-earth-doped inorganic phosphors are widely used in a range of applications, such as, medical

✉ P. D. Sahare
pdsahare@yahoo.co.in

✉ Nandkumar T. Mandlik
nandkumar.mandlik@fergusson.edu; ntmandlik@gmail.com

[1] Department of Physics and Astrophysics, University of Delhi, Delhi 110007, India

[2] Department of Physics, Fergusson College (Autonomous) Pune, Affiliated to Savitribai Phule Pune University, Pune 411004, India

[3] Department of Physics, Savitribai Phule Pune University, Pune 411007, India

dosimetry, radiation dosimetry, dose mapping, lamp industry, X-ray imaging, colour display, radiological incidents and imaging, etc. [19]. Rare-earth ion doped phosphors have been widely studied for their superior luminescence properties. Doped alkaline-earth borates such as $MgB_4O_7$:Dy,Na [7], $CaB_4O_7$:Dy,Eu [8, 9], $SrB_4O_7$:Cu [10], $SrB_4O_7$:Dy [11], $SrB_4O_7$:Eu,Gd [12], $SrB_4O_7$:Eu,Tb [13] $SrB_4O_7$:$Sm^{2+}$ [14] are some of the most promising materials for individual doses owing to their high sensitivity and, in certain cases, their TL tissue-like properties for radiation absorption. To be more specific, the luminescent properties of europium-ion doped phosphors have been studied expansively. SBO on doping with rare earth ions [20–22] is no exception and has been used as a host medium for several luminescence applications. The synthesis of rare earth doped SBO phosphors has been carried out by using various techniques, such as, combustion method, Kyropoulos method, micro-pulling-down method, Pechini-type sol–gel method, conventional melt-quenching method and so on [23–26]. Due to simplicity and larger product formation, solid state diffusion method was widely used for the synthesis of SBO. Also, this method provides the advantage for controlling the particle size of the sample from micro to nano scale.

In this work, $SrB_4O_7$:$Eu^{3+}$ microphosphor has been synthesized by using solid state diffusion method and its thermoluminescence (TL) and photoluminescence (PL) properties were studied. The influence of impurity doping concentrations and that of annealing and quenching temperatures on structural, morphological, compositional and luminescent (TL) properties of the $SrB_4O_7$:$Eu^{3+}$ microphosphor has also been studied. Moreover, the investigation of the formation of different local energy levels due to the presence of the impurity in different ionic forms was carried out using photoluminescence (PL) technique. The phosphor material in the microcrystalline form was irradiated with different gamma radiation doses using $^{60}$Co gamma source and its thermoluminescence (TL) dosimetry study was carried out. These were the absorbed doses of the radiation. The exact peak positions and the number of peaks of TL glow curve were confirmed by $T_m$-$T_{stop}$ method. The TL glow curve was also deconvoluted by using Computerized Glow Curve Deconvolution (CGCD) method and the trapping parameters, such as, order of kinetics, activation energy, frequency factor, were determined.

## Experimental

### *Synthesis of $SrB_4O_7$:$Eu^{3+}$*

$SrB_4O_7$:$Eu^{3+}$ microphosphor synthesized by using solid state diffusion method. In this method Europium chloride ($EuCl_3$) (0.2 mol%) and Strontium carbonate ($SrCO_3$) are mixed in distilled water and stirred on a magnetic stirrer at room temperature (RT) for 30 min. Few drops of concentrated hydrochloric acid (HCl) were added into the solution to dissolve/disperse the $EuCl_3$ compound completely. This solution was further heated in an oven to form the powder by removing all water molecules. The powder thus formed was then transferred to an agate mortar with addition of boric acid ($H_3BO_3$) and grinded for 20 h. After grinding, the mixture was annealed at 500 °C for 2 h in muffle furnace. With the help of sieves, particles with size in the range of 90–120 µm were collected and further annealed and quenched at different temperatures (in the range of 400–900 °C) for 2 h. Finally, the microcrystalline samples were irradiated with different gamma radiation doses by using $^{60}$Co gamma source. Likewise, to study the effect of Eu concentration on SBO structure, synthesis of $SrB_4O_7$:$Eu^{3+}$ microphosphor with different concentrations of europium (0.1–1.0 mol%) was carried out by using same the procedure. Figure 1 shows schematic diagram for synthesis of $SrB_4O_7$:$Eu^{3+}$ microphosphor by solid state diffusion method.

### Characterization techniques

The structural characterization of prepared sample was carried out by XRD using Cu-target (Cu-Kα = 1.54 Å) on Bruker AXS D-8 Advance X-ray Diffractometer. The morphological study was done by scanning electron microscope (SEM) attached with energy-dispersive X-ray spectrometer (EDS) (JEOL JSM-6360A). The Photoluminescence (PL) excitation and emission spectra were recorded using Horiba FluoroLog Spectrophotometer (Horiba Inc., Worldwide). For PL measurements, same weight of powder sample (~ 50 mg) was used for all the measurements. For TL measurement, $SrB_4O_7$:$Eu^{3+}$ powder samples were exposed to gamma rays from the $^{60}$Co radioactive source for various doses. The TL glow curves were recorded using a computerized Nucleonix TLD Reader (Model TL1009I), by taking ~ 5.0 mg of the sample each time and heating it with a constant rate of 5 °$Cs^{-1}$ with the help of a temperature programmer and controller.

## Results and discussion

### X-ray diffraction spectroscopy

The XRD patterns of the $SrB_4O_7$:$Eu^{3+}$ (0.2 mol%) as prepared and annealed at different temperatures (400 ºC and 500 ºC) are shown in Fig. 2. The XRD peaks of the sample shows the orthorhombic phase (space group $Pmn2_1$(31)) with lattice parameters are, a = 3.9190 Å, b = 4.4632 Å and c = 10.8788 Å which matches well with the same found in

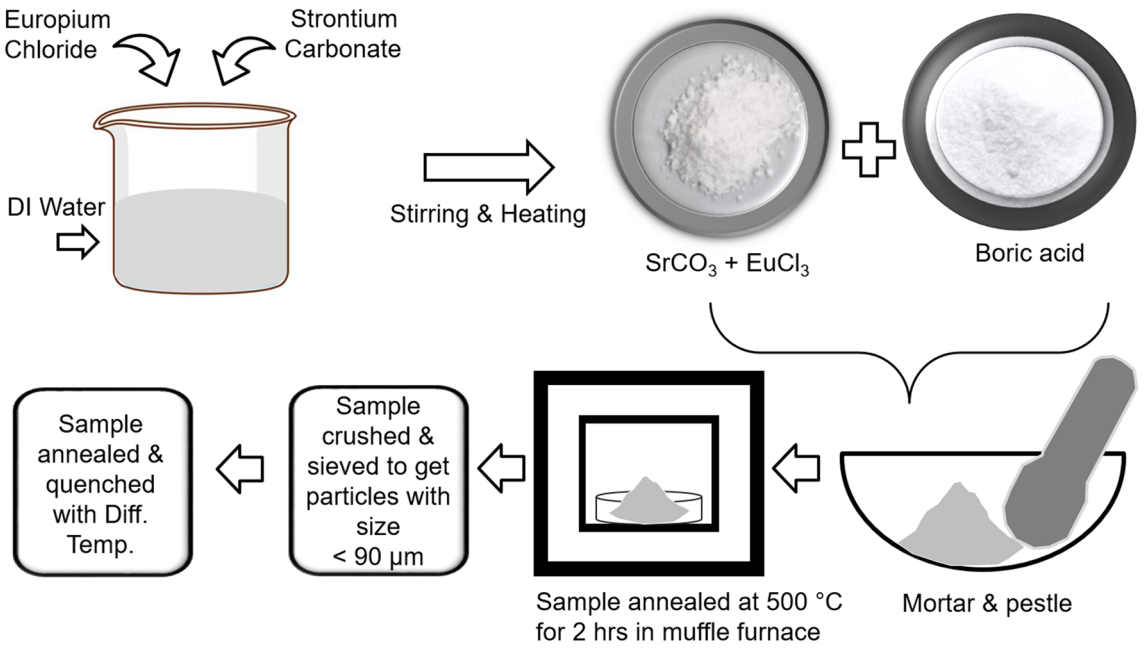


**Fig. 1** Schematic diagram for synthesis of $SrB_4O_7$:$Eu^{3+}$ microphosphor by using solid state diffusion method

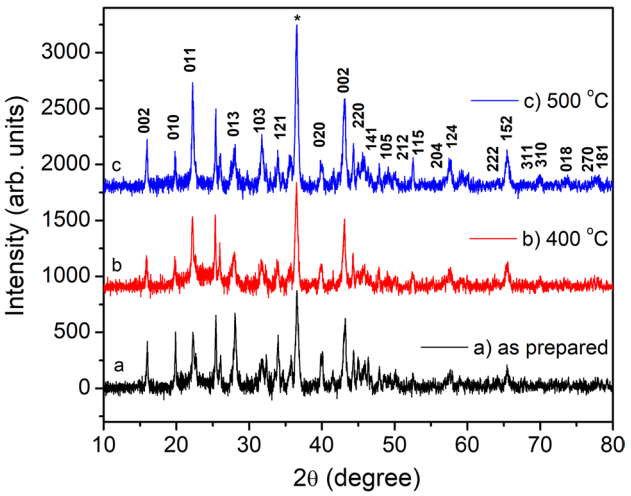


**Fig. 2** X-ray diffraction patterns of $SrB_4O_7$:$Eu^{3+}$ (0.2 mol%) microphosphor **a** as prepared, **b** annealed at 400 °C, **c** annealed at 500 oC for 2 h

JCPDS file # 71–2191. A sharp peak at ~ 36º may be due to unreacted strontium carbonate during the chemical reaction.

## Scanning electron microscopy (SEM) and energy dispersive spectroscopy (EDS)

The morphological study of the prepared sample was carried out using scanning electron microscope technique. Figures 3 a-c show SEM images of as prepared $SrB_4O_7$:$Eu^{3+}$ (0.8 mol%) microphosphor and Figs. 3 d–f show SEM images of the same phosphor but annealed and quenched at 700 ° for 2 h. The SEM results show, the prepared samples have irregular shaped particles with average size around 20–30 µm.

The elemental compositional analysis of $SrB_4O_7$:$Eu^{3+}$ microphosphor was obtained from the energy dispersive spectroscopy (EDS). Figures 4 a and b show EDS of as prepared and annealed $SrB_4O_7$:$Eu^{3+}$ (0.8 mol%) microphosphor, respectively. It reveals that they are mainly composed of Sr, B, and O with a small amount of Eu. The EDS patterns confirm the presence of Eu in the $SrB_4O_7$:$Eu^{3+}$ powder and percentage of the impurity is very nearly equal to the doped value of the impurity (Eu). The Figs. 4 c-f show the elemental mapping of Sr, B, O and Eu elements in $SrB_4O_7$:$Eu^{3+}$ (0.8 mol%) microphosphor (annealed and quenched at 700 °C). It was found that the components (i.e., Sr, B, O, and Eu) were evenly distributed among the particles. Table 1 represents the atomic percentage of the compositional elements in the $SrB_4O_7$:$Eu^{3+}$ sample.

## Photoluminescence

The photoluminescence (PL) properties of the $SrB_4O_7$-$Eu^{3+}$ (0.2 mol%) sample annealed and quenched at 700 °C was carried out by PL excitation and emission spectra, with maintaining equal amount of sample during each measurements. Figure 5 shows the excitation spectra (recorded at 420 nm and 615 nm emission wavelengths) of $SrB_4O_7$:$Eu^{3+}$ (0.2 mol%) microphosphor annealed and quenched at 700 °C for 2 h obtain in the range 200–600 nm. It is very difficult

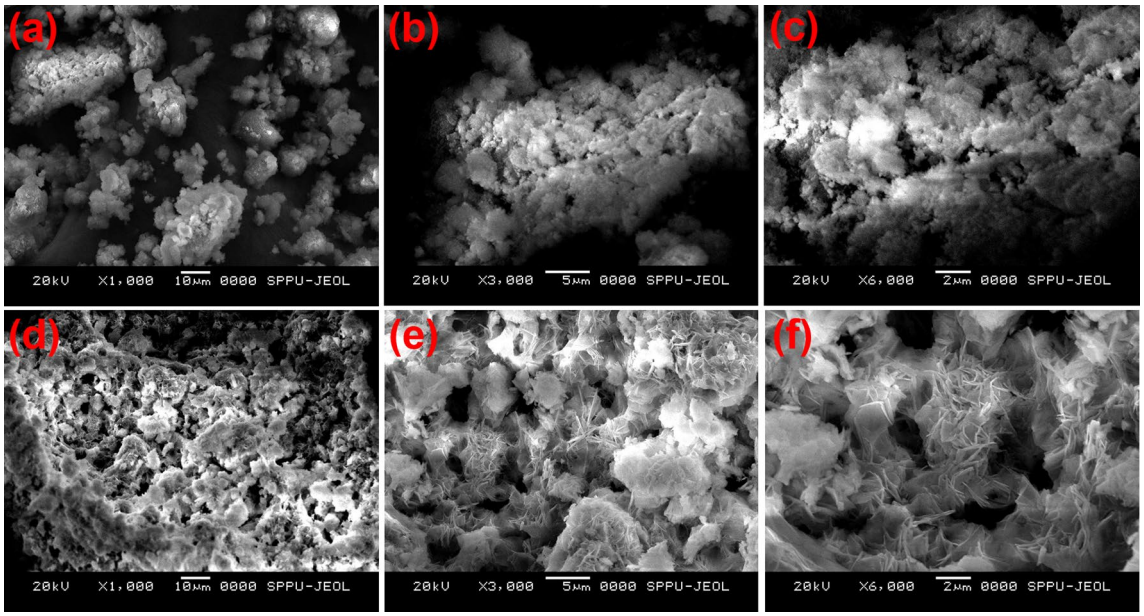


**Fig. 3** SEM images of $SrB_4O_7:Eu^{3+}$ (0.8 M %) microphosphor, **a**-**c** as prepared, **d**-**f** annealed at 700 °C for 2 h

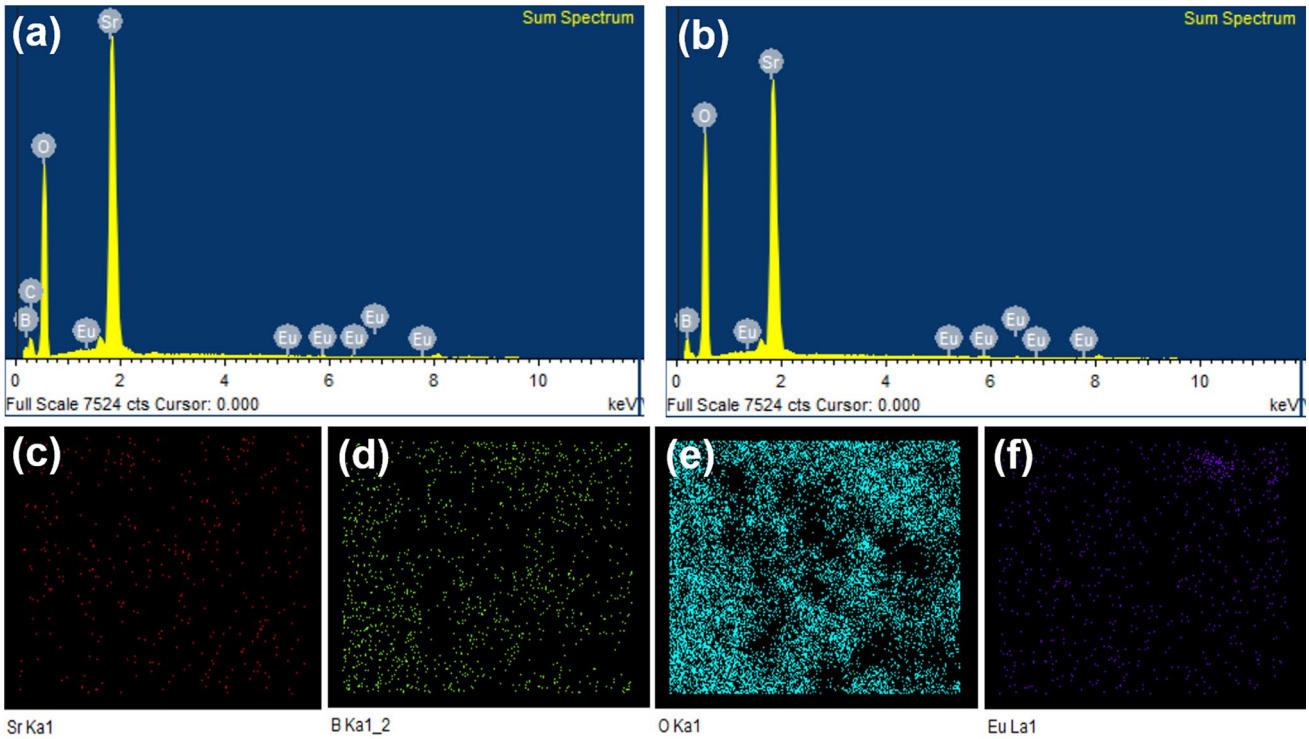


**Fig. 4** EDS report micrographs of $SrB_4O_7:Eu^{3+}$ (0.8 mol%) microphosphor **a** as prepared, **b** annealed at 700 °C for 2 h, **c**-**f** elemental mapping of $SrB_4O_7:Eu^{3+}$ (0.8 M %) microphosphor (annealed and quenched at 700 °C)

to observe different distinct peaks in the excitation spectrum. It shows two visible shoulders at ~ 300 nm and 358 nm with corresponding to f-d transition ($4f^6 5d$- $4f^7$) ($^8S_{7/2}$) of $Eu^{2+}$ ions in the host lattice [27]. These transitions arise from divalent europium ion ($Eu^{2+}$) in the host lattices. A less intense peaks at ~ 250 nm and hidden peak at 300 nm are observed which corresponds to 5d orbital splitting in $t_{2g}$ and $e_g$ compounds, respectively [28, 29]. These transition

**Table 1** Compositional study of Strontium (Sr), Boron (B), Oxygen (O) and Europium (Eu) in $SrB_4O_7:Eu^{3+}$ (0.8 mol%) microphosphor

| Sr. no | Compound | Strontium (Sr) atomic % | Boron (B) atomic % | Oxygen (O) atomic % | Europium (Eu) atomic % |
|---|---|---|---|---|---|
| 1 | $SrB_4O_7:Eu^{3+}$ (0.8 mol%) as prepared | 4.42 | 6.98 | 61.58 | 0.02 |
| 2 | $SrB_4O_7:Eu^{3+}$ (0.8 mol%) annealed and quenched at 700 ℃ for 2 h | 3.89 | 34.70 | 61.37 | 0.05 |

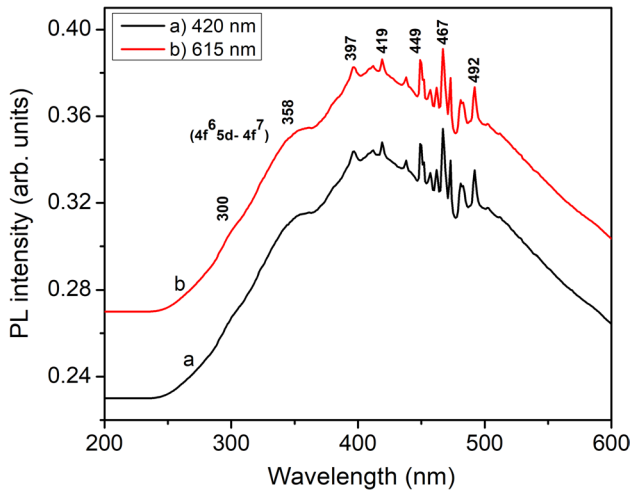


**Fig. 5** Excitation spectra of $SrB_4O_7:Eu^{3+}$ (0.2 mol%) microphosphor annealed at 700 °C for 2 h with emission at **a** 420 nm and **b** 615 nm

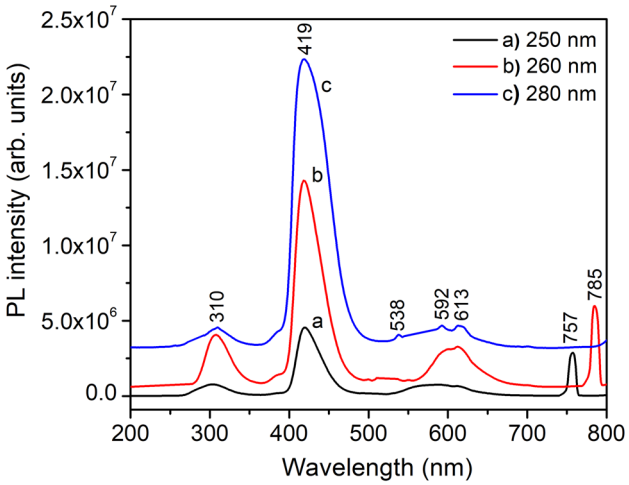


**Fig. 6** Emission spectra of $SrB_4O_7:Eu^{3+}$ (0.2 mol%) microphosphor with excitation at **a** 250 nm, **b** 260 nm and **c** 280 nm

bands in the spectral range 250–360 nm are connected with energy transfer between $Eu^{2+}$ and $Eu^{3+}$ [30]. In the range 450–550 nm, excitation peaks are assigned to the $^7F_0$-$^5H_3$, $^7F_0$-$^5D_4$, $^7F_0$-$^5L_7$, $^7F_0$-$^5F_6$, and $^7F_0$-$^5d_3$ intra-configurational 4f-4f transitions of $Eu^{3+}$, respectively [30]. Other noticeable peaks were observed at higher wavelength region between 360 and 500 nm range. These peaks are appearing due to inter-configurational *f-f* transitions of $Eu^{3+}$ ions resulting from excitation of the $Eu^{3+}$ ground state to the higher levels of $4f^6$ arrangements, some of them assigns as $^7F_0$—$^5L_6$ (394 nm), $^7F_0$—$^5D_3$ (419 nm), and $^7F_0$—$^5D_2$ (467 nm). For 420 nm and 615 nm emission wavelengths, the excitation spectra look very much similar with very slight shifts in the peak positions and small changes in their relative intensities with respect to each other.

The emission spectra of $SrB_4O_7:Eu^{3+}$ (0.2 mol%) microphosphor annealed and quenched at 700 °C for 2 h was recorded in the range of 200–800 nm with different excitation wavelength (250 nm, 260 nm, and 280 nm), shown in Fig. 6. It is observed that the PL spectra shows a blue emission bands appearing at around 310 nm and 420 nm which could be attributed for $Eu^{2+}$ (4*f*—5d) transitions [31]. Some other small peaks in the range 500–710 nm were recognized as transitions of $Eu^{3+}$ ions from $^5D_0$ – $^7F_J$, (J = 0, 1, 2, 3 and 4). These appearances of peaks between 300 to 420 nm suggest the existence of $Eu^{2+}$ ions in different surrounding

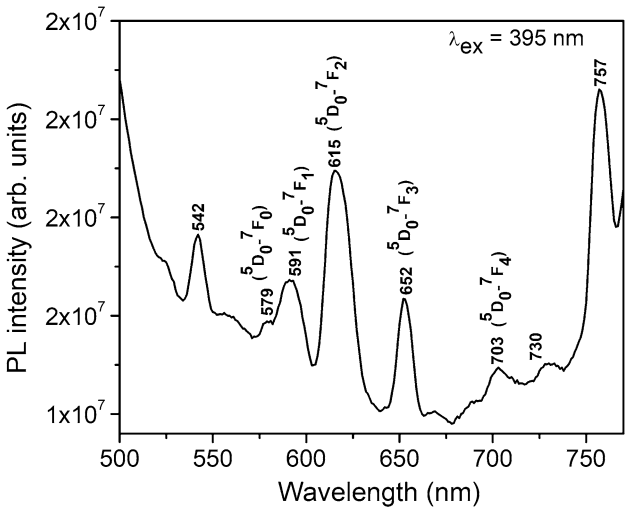


**Fig. 7** Emission spectra of $SrB_4O_7:Eu^{3+}$ (0.2 mol%) microphosphor annealed at 700 °C for 2 h with λex = 395 nm

environment. Figure 7 shows the emission spectrum of the $SrB_4O_7:Eu^{3+}$ (0.2 mol% sample) microphosphor annealed and quenched at 700 ºC for 2 h with excitation at 395 nm. The emission spectrum consists of several prominent peaks at 579 nm, 591 nm, 615 nm, 652 nm, and 703 nm which were attributed to $^5D_0$-$^7F_0$, $^5D_0$-$^7F_1$, $^5D_0$-$^7F_2$, $^5D_0$-$^7F_3$, and

$^5D_0$-$^7F_4$, (i.e., $^5D_0$-$^7F_J$, J = 0, 1, 2, 3 and 4), respectively, for $Eu^{3+}$ ions. A peak Centered at 615 nm represents the red emission from $^5D_0$–$^7F_2$ transition corresponds to electric dipole transition, while peak at 591 nm from $^5D_0$–$^7F_1$ is a typical magnetic dipole transition [27]. It was initially thought that as the source of impurity consists of $Eu^{3+}$ ions they might have been incorporated inside the material in this form only but the PL studies show that they are in different ionic forms, plausibly, due to charge compensation in different surrounding atmosphere or there might be some redox reactions occurring inside the material on annealing.

## Thermoluminescence glow curves

The $SrB_4O_7$:$Eu^{3+}$ (0.2 mol%) microphosphor, annealed and quenched at different temperature (400–900 °C) for 2 h, exposed to 100 Gy, 1.0 kGy and 6.0 kGy of gamma radiation doses from $^{60}$Co source. Figures 8 9 and 10 show TL glow curves of $SrB_4O_7$:$Eu^{3+}$ (0.2 mol%) microphosphor; annealed and quenched at different temperatures; exposed to 100 Gy, 1.0 kGy and 6.0 kGy; respectively. Figure 11 represents the graph of total TL intensity vs. annealing temperature for $SrB_4O_7$:$Eu^{3+}$ (0.2 mol%) microphosphor exposed to 100 Gy, 1.0 kGy and 6.0 kGy of gamma radiation doses. In these figures, the ordinate value needs to be multiplied by the number shown near the corresponding curves to get the relative intensities. It is observed that TL intensity increases with annealing temperature maximum up to 700 °C and then starts decreasing on annealing at higher temperatures. This might be due to the impurity aggregation at low temperatures and acting as self-quenchers [32]. Also, during synthesis, europium chloride and strontium carbonate were mixed in distilled water, therefore; some water molecules are present in sample and act as quenchers for TL. At higher temperatures they disperse making maximum luminescence centres at around 700 °C. If sample annealed beyond 700 °C, there could be more complexes formation resulting in TL quenching [32]. It also shows that TL glow curve changes with annealing temperature, it may be due to phase change of $SrB_4O_7$:$Eu^{3+}$ phosphor or conversion of $Eu^{3+}$ to $Eu^{2+}$, these results change in the energy level structure and hence

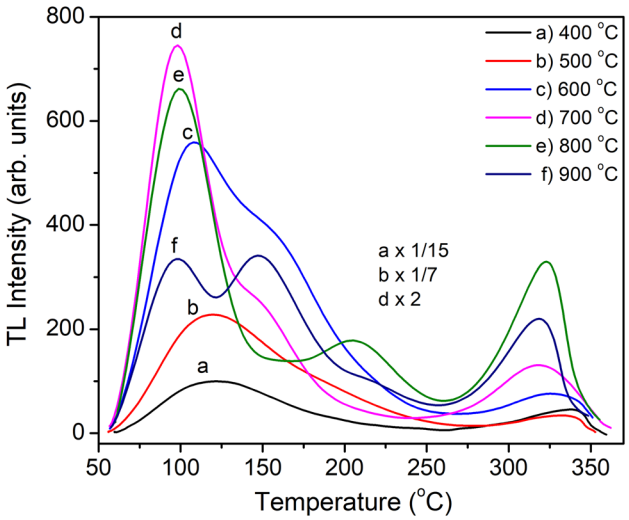


**Fig. 9** TL glow curves of $SrB_4O_7$:$Eu^{3+}$ (0.2 mol%) microphosphor annealed at different temp for 2 h and exposed to 1 kGy of gamma doses from $^{60}$Co source. The ordinate is to be multiplied by the numbers at the curves to get the relative intensities

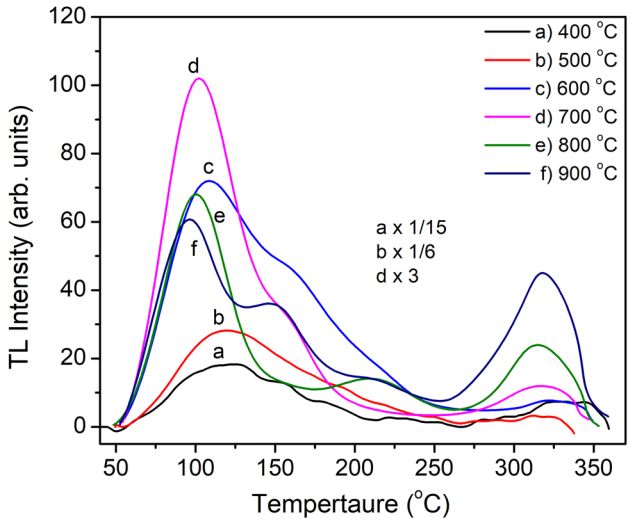


**Fig. 8** TL glow curves of $SrB_4O_7$:$Eu^{3+}$ (0.2 mol%) microphosphor annealed at different temp for 2 h and exposed to 100 Gy of gamma doses from $^{60}$Co source. The ordinate is to be multiplied by the numbers at the curves to get the relative intensities

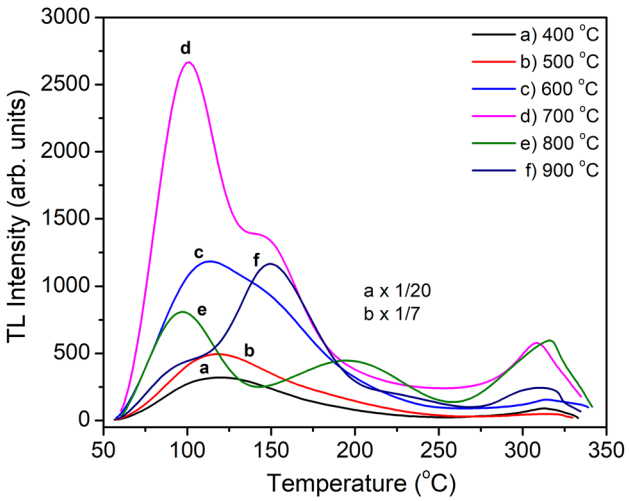


**Fig. 10** TL glow curves of $SrB_4O_7$:$Eu^{3+}$ (0.2 mol%) microphosphor annealed at different temp for 2 h and exposed to 6 kGy of gamma doses from $^{60}$Co source. The ordinate is to be multiplied by the numbers at the curves to get the relative intensities

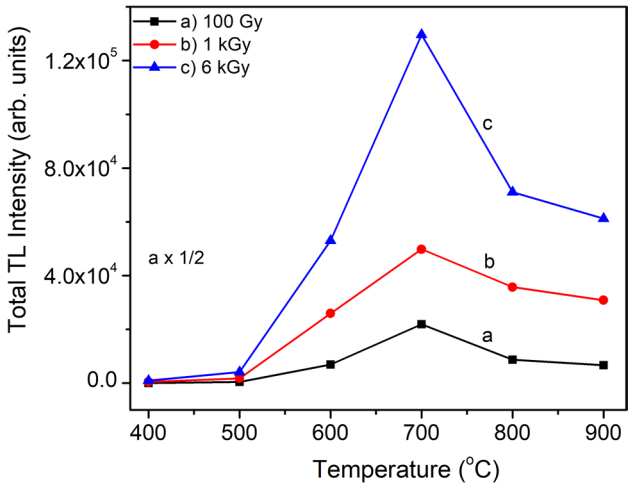


**Fig. 11** Graph of total TL intensity vs. annealing temperature of $SrB_4O_7$:$Eu^{3+}$ (0.2 mol%) microphosphor exposed to **a** 100 Gy, **b** 1 kGy, and **c** 6 kGy of gamma dose from $^{60}Co$. The ordinate is to be multiplied by the numbers at the curves to get the relative intensities

there may be corresponding changes in the TL glow curve [33]. Bakshi et. al. [34] mentioned that the change in TL glow curve structure is attributed to the diffusion of atmospheric oxygen at high temperatures. This may form some clusters of strontium oxide SrO and change the glow curve structure.

The TL glow curve of $SrB_4O_7$:$Eu^{3+}$ (0.2 mol%) microphosphor, annealed and quenched at 700 °C for 2 h was found to be the most sensitive to radiation amongst the samples annealed at different temperatures (optimized for impurity concentrations and annealing temperatures) and was used for further studies. It was further exposed to 100 Gy (Fig. 8), apparently shows major peak (high intensity) at ~ 102 °C, a hump at ~ 163 °C and a small peak (low intensity) at ~ 317 °C. If it is exposed to 1.0 kGy (Fig. 9), TL glow curve apparently shows major peak at ~ 98 °C, a hump at ~ 154 °C and a small peak (low intensity) at ~ 319 °C and for 6.0 kGy (Fig. 10); TL glow curve shows major peak (high intensity) at ~ 101 °C, a hump at ~ 147 °C and a small peak (low intensity) at ~ 308 °C. Thus, the shifting of TL peak position is observed with dose. This shifting of TL peak with dose is due to the disorganization of trapping centers (TCs)/luminescent centers (LCs) [35, 36]. The TL peaks are may be a first order, second order or general order of kinetics. In a second-order or general order reaction released electrons are re-trapped before they recombine. This results in the shift in the peak temperatures of a glow curve with dose as well as with the heating rate. Thus, a TL peak may be second or general order of kinetics [36, 37]. To find the order of kinetics and activation energy, deconvolution of glow curve is necessary. The peaks are deconvoluted (in the following section *Deconvolution of TL glow curves*) and it is verified that the peaks are of general order (Table 2).

**Table 2** Trapping parameters of $SrB_4O_7$-Eu phosphor for 1.0 kGy of γ –dose

| Peak | Peak temp. $T_m$ ($^0C$) | Peak temp. $T_m$ (K) | Order of kinetics (b) | Trap depth E (eV) | Frequency factor S ($s^{-1}$) |
|---|---|---|---|---|---|
| *a* | 87.49 | 360.49 | 1.8 | 0.89 | $1.32\times10^{12}$ |
| *b* | 138.20 | 411.20 | 1.3 | 0.43 | $2.4\times10^{4}$ |
| *c* | 318.52 | 591.52 | 1.3 | 0.46 | $1.2\times10^{10}$ |

The synthesis of $SrB_4O_7$ microphosphor doped with different mole concentrations of Eu in the range of 0.1–1.0 mol% with annealing and quenching at 700 °C for 2 h was carried out for studying the behavior of dopant on the luminescent properties of the sample. Figure 12 represents the TL glow curves of $SrB_4O_7$:$Eu^{3+}$ microphosphor doped at different molar concentrations of Eu ions, annealed and quenched at 700 °C for 2 h, and exposed to 1.0 kGy of gamma dose from $^{60}Co$ source. Figure 13 shows the total TL intensity vs. different Eu concentrations (0.1–1.0 mol%) of $SrB_4O_7$:$Eu^{3+}$ microphosphor. The effect of impurity concentrations on the TL sensitivity attributed to the concentration quenching. The luminescence of a material is very sensitive to the impurity concentration. If the impurity concentration is too high, they may act as self-quenchers by causing nonradiative cross transitions resulting in quenching of the luminescence [32]. In $SrB_4O_7$:$Eu^{3+}$ microphosphor, the optimum impurity concentration was found for 0.2 mol% of europium doping,

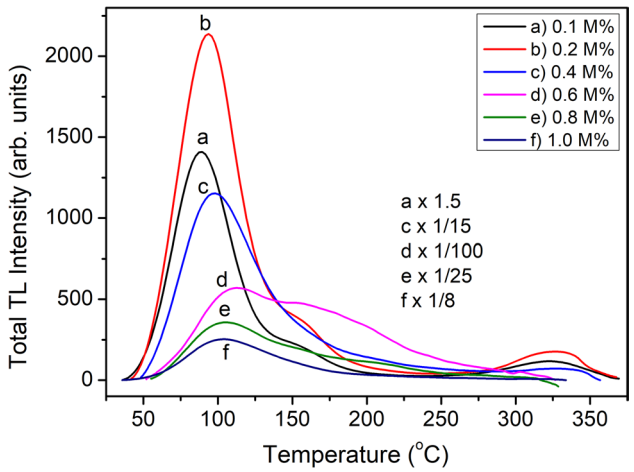


**Fig. 12** TL glow curve of $SrB_4O_7$:$Eu^{3+}$ microphosphor with different Eu concentrations (0.1 to 1 mol%) annealed/quenched at 700 °C for 2 h and exposed to 1 kGy of gamma dose from $^{60}Co$. The ordinate is to be multiplied by the numbers at the curves to get the relative intensities

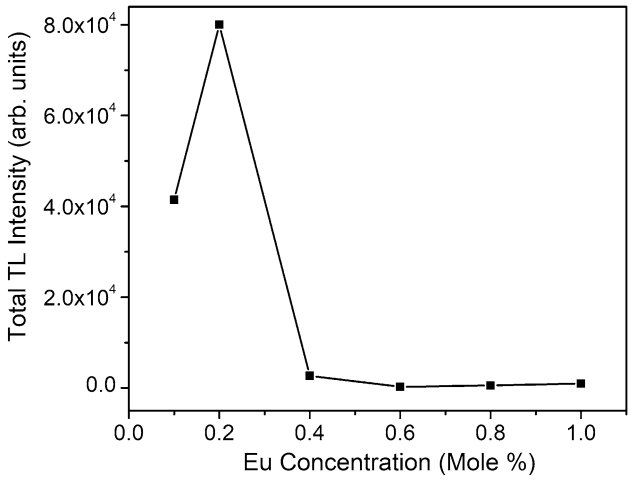


**Fig. 13** Graph of total TL intensity vs. different Eu concentrations (0.1 to 1 mol%) of $SrB_4O_7:Eu^{3+}$ microphosphor annealed and quenched/quenched at 700 °C for 2 h and exposed to 1 kGy of gamma dose from $^{60}Co$

and above this quantity the TL intensity starts decreasing (Fig. 13).

## Comparison with standard phosphors

The intensity of the newly developed $SrB_4O_7:Eu^{3+}$ phosphor was compared with that of some standard (commercially available) TLD phosphors, such as, $CaSO_4$:Dy (TLD-900) and LiF: Mg,Cu,P (TLD-700H). The results are as shown in Fig. 14. It could be seen that the first peak (88 °C with a shoulder at 138 °C) of the $SrB_4O_7:Eu^{3+}$ phosphor is highly sensitive (approx. twice that of TLD-900 and around 1.33 times that of TLD-700H) but it is at quite low temperature, mostly (around 70%) fades in 48 h and therefore, it is not very useful for dosimetry. However, the isolated high temperature peak (318 °C) is quite stable and could be used. The relative sensitivity of this peak for 10 Gy dose is of the same order (~0.5 times than that of TLD-900 and ~0.42 that of TLD-700H considering the peak heights of the dosimetry peaks). As it is appearing at quite high temperature as compared to the standard phosphors and thus shows better stability.

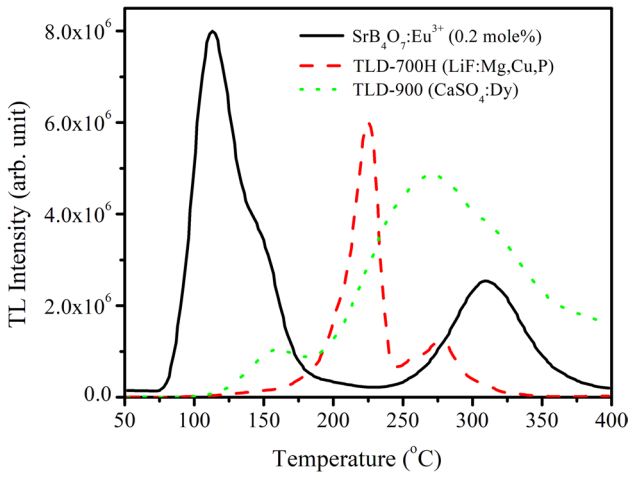


**Fig. 14** Comparison of the sensitivity of the $SrB_4O_7:Eu^{3+}$ TLD phosphor with at of the commercially available $CaSO_4$:Dy and LiF:Mg,Cu,P (Harshaw TLD 700H) phosphors

## Dose response

The dose vs. TL intensity plots (dose response) for the SrB4O7:Eu (0.2 mol%) is shown in Fig. 15. From the figure it could be observed that the response of the complete glow curve as well as individual peaks (peak 1 appearing at around 88 °C and another peak appearing at around 138 °C) is very much linear (little sublinear) and unlike in commercially available phosphors (which saturate around 100 Gy) it saturates at around 2.0 kGy except for peak 3 which becomes supralinear after 1.0 kGy before saturating at around 10 kGy.

## Reusability

The $SrB_4O_7:Eu^{3+}$ phosphor under investigation was irradiated for 100 Gy dose and TL was taken. The same sample was annealed at 700 °C for 2 h and again TL was recorded after irradiating for the same dose. The procedure was repeated several times (at least 25 times). The results given in Fig. 14 show excellent reusability, the material is quite stable even for high doses and not much radiation hardening was observed (Fig. 16).

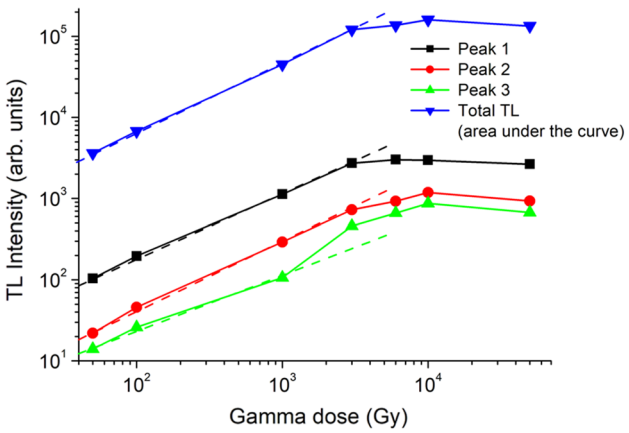


**Fig. 15** Dose response of the $SrB_4O_7:Eu^{3+}$ (0.2 mol%) TLD phosphor

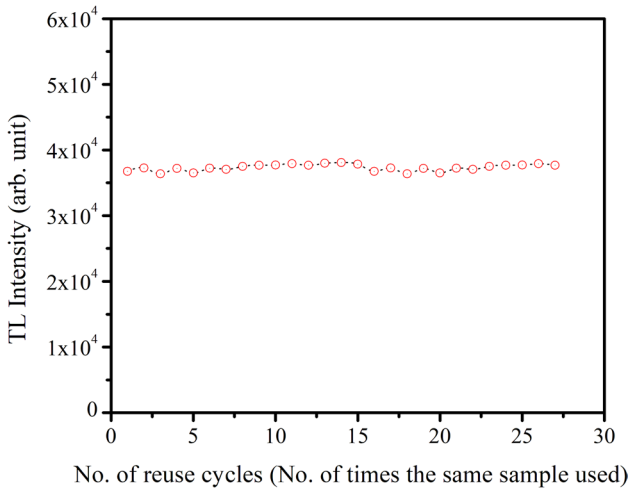


**Fig. 16** Reusability of the $SrB_4O_7:Eu^{3+}$ (0.2 mol%) TLD phosphor

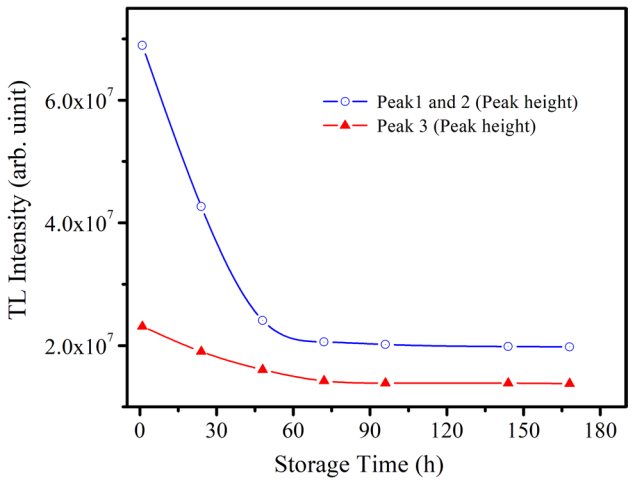


**Fig. 17** Fading of the $SrB_4O_7:Eu^{3+}$ (0.2 mol%) TLD phosphor

## Fading

Several samples (~ 5.0 mg each) of the phosphor material was irradiated to 10 Gy dose and stored at room temperature (27 °C) in dark. The TL was recorded at different intervals of time by taking out one sample at a time. It could be seen from the TL intensity vs. storage time plots as shown in Fig. 17 that there is about 70% fading of the first peak (88 °C along with a shoulder at around 138 °C), however, that of the high temperature peak is only around 5% in approx. over a week's time.

### $T_m$-$T_{stop}$ method

To find the trapping parameters such as, order of kinetics, activation energy, frequency factor, etc., deconvolution of the TL glow curve is necessary. Before doing the deconvolution the exact peak positions and the number of TL glow peaks were confirmed by $T_m$-$T_{stop}$ method. The individual peaks were resolved by $T_m$-$T_{stop}$ method suggested by McKeever [38]. The $SrB_4O_7:Eu^{3+}$ (0.2 mol%) microphosphor (annealed at 700 °C for 2 h) was irradiated by 1.0 kGy dose of γ -rays from $Co^{60}$ source. The 5.0 mg sample was heated with a linear rate (5 $°Cs^{-1}$) to a temperature $T_{stop}$ corresponding to a position on the low-temperature tail of the first glow peak.

The sample was then cooled rapidly to room temperature and then re-heated at the same linear rate in order to record all of the remaining TL glow-curve. The position of the first maximum ($T_m$) in the glow-curve was noted. Again, a freshly irradiated 5.0 mg sample was heated up to new $T_{stop}$ temperature, it was cooled to room temperature, TL was taken and the position of $T_M$ was recorded. The whole process was repeated using a different value of $T_{stop}$ each time. The $T_{stop}$ was increased each time by 5 °C and the corresponding $T_M$ value was noted on each occasion. The $T_m$ vs. $T_{stop}$ values were plotted (Fig. 14) to obtain a staircase type of curve where the $T_M$ values corresponding to the stairs (horizontally flat portions of the curve) are the respective maximum peak temperatures. The three peaks were revealed in TL glow curve $SrB_4O_7:Eu^{3+}$ (0.2 mol%) microphosphor at positions 88, 138 and 318 °C.

### Deconvolution of TL glow curves

For the deconvolution of TL glow curves, $SrB_4O_7:Eu^{3+}$ (0.2 mol%) microphosphor (annealed at 700 °C for 2 h) was irradiated by 1.0 kGy dose of γ -rays from $^{60}Co$ source. Initially the peak positions were confirmed by $T_m$-$T_{stop}$ method. The three peaks were revealed at positions 88, 138 and 318 °C. By keeping these peak positions TL glow curve was deconvoluted. The Computerized Glow Curve Deconvolution (CGCD) curve fitting was done using glow curve deconvolution (GCD) functions (Eqs (1) and (2), suggested by Kitis [39], for general and first order kinetics glow curves, respectively. For kinetic analysis the experimentally obtained TL glow curve was fitted with CGCD method which was given by Pagonis et. al. [40].

For General order

$$I(T) = I_m b^{\left(\frac{b}{b-1}\right)} exp\left(\frac{E}{kT}\frac{T-T_m}{T_m}\right)\left[(b-1)\frac{T^2}{T_m^2}\left(1-\frac{2kT}{E}\right)exp\left(\frac{E}{kT}\frac{T-T_m}{T_m}\right)+1+(b-1)\frac{2kT_m}{E}\right]^{\frac{b}{b-1}} \quad (1)$$

For First order:

$$I(T) = I_m exp\left[1+\frac{E}{kT}\frac{T-T_m}{T_m}-\frac{T^2}{T_m^2}exp\left(\frac{E}{kT}\frac{T-T_m}{T_m}\right)\left(1-\frac{2kT}{E}\right)-\frac{2kT_m}{E}\right] \quad (2)$$

Here, *I (T)* is the TL intensity at temperature *T* (K), $I_m$, the maximum peak intensity, $T_m$, is the temperature corresponding to maximum peak intensity $I_m$, *E*, trap depth or the thermal activation energy (eV) needed to free the trapped electrons, *b*, order of kinetics, *k*, the Boltzmann's constant ($8.6\times10^{-5}$ eVK$^{-1}$).

The frequency factor ***s*** is obtained from the following equations.

For general order:

$$s = \frac{\beta E}{kT_m^2\left(1+(b-1)\frac{2kT_m}{E}\right)}\exp\left(\frac{E}{kT_m}\right) \quad (3)$$

For first order:

$$s = \frac{\beta E}{kT_m^2}\exp\left(\frac{E}{kT_m}\right) \quad (4)$$

where $\beta$ is the linear heating rate and *b* is the order of kinetics.

The de-convoluted TL curves and the theoretical curve fitting with the experimental after convolution are shown in Fig. 15. The goodness of the fitting, i.e., figure of merit (FOM), is found to be less than 1%. This shows that experimental and theoretical glow curves are in good agreement and very much overlapping on either side. The deconvolution of the experimental curve has revealed three peaks at 88, 138 and 318 °C.

#### Calculation of trapping parameters by Chen's formulae

To verify further, the thermal activation energy (E) and order of kinetics (b) of the deconvoluted glow peaks were calculated using Chen's set of empirical formulae [41] as follows.

$$E_\alpha = c_\alpha\left(\frac{kT_m^2}{\alpha}\right) - b_\alpha\left(2kT_m\right) \quad (5)$$

with

$\alpha = \tau, \delta, \omega,$

$\tau = T_m - T_1, \delta = T_2 - T_m, \omega = T_2 - T_1,$

$c_\tau = 1.51 + 3.0\left(\mu_g - 0.42\right),$

$c_\delta = 0.976 + 7.3\left(\mu_g - 0.42\right),$

$c_\omega = 2.52 + 10.2\left(\mu_g - 0.42\right),$

$b_\tau = 1.58 + 4.2\left(\mu_g - 0.42\right),$

$b_\delta = 0,$

$b_\omega = 1.$

To determine the order of kinetic, the form factor was calculated by using the equation,

$$\mu_g = \frac{T_2 - T_m}{T_2 - T_1} \quad (6)$$

Theoretically the form factor, $\mu_g$, ranges between 0.42 and 0.52, the value is close to 0.42 for first order kinetics and 0.52 for second order kinetics. To determine the general order of kinetics (other than first or second order), use of the correlation between order of kinetics (*b*) and the form factor ($\mu_g$) given by Chen was made [42]. The values calculated by Chen's set of equations are very well matches with the values calculated by CGCD program using Kitis functions. As discussed earlier, (in the section *'Thermoluminescence Glow Curves)*, the shift in the TL peak position with dose indicates that the peak is not of first order; it may be second or general order of kinetics. It is also confirmed by deconvolution of TL glow curve. The order of kinetics of first peak is 1.8, and that of second and third peak is 1.3 (Table 2), i.e., retrapping taking place in $SrB_4O_7$:$Eu^{3+}$ (0.2 mol%) microphosphor. The thermal activation energy or trap depth (eV) needed to free the trapped electrons are given Table 2. The values of frequency factor or attempt to escape factor vary from $10^4$–$10^{12}$ s$^{-1}$.

## Conclusions

The $SrB_4O_7$:$Eu^{3+}$ microphosphor was synthesized by solid state diffusion method. It exhibits orthorhombic structure (space group $Pmn2_1(31)$) and lattice parameters a = 3.9190 Å, b = 4.4637 Å, c = 10.8788 Å. The compositional studies determine the presence of strontium,

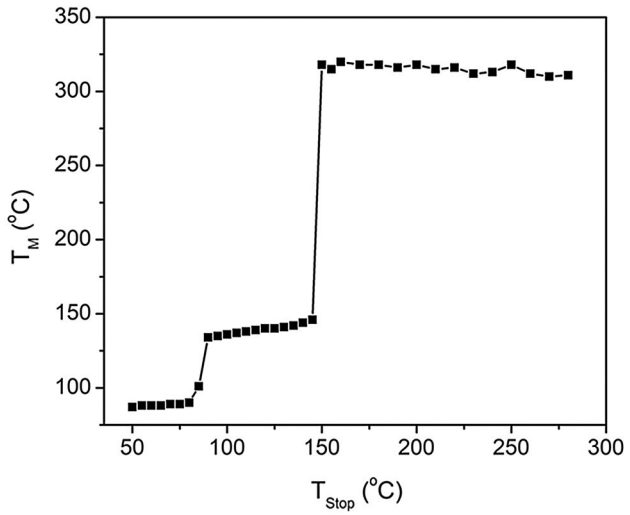


**Fig. 18** A typical $T_m$–$T_{stop}$ plot for the $SrB_4O_7$:$Eu^{3+}$ (0.2 mol%) microphosphor (annealed at 700 °C for 2 h) exposed to 1.0 kGy gamma dose from $^{60}$Co source. In the staircase kind of curve, the $T_m$ corresponding to the stairs (horizontally flat portions of the curve) are the respective maximum peak temperatures

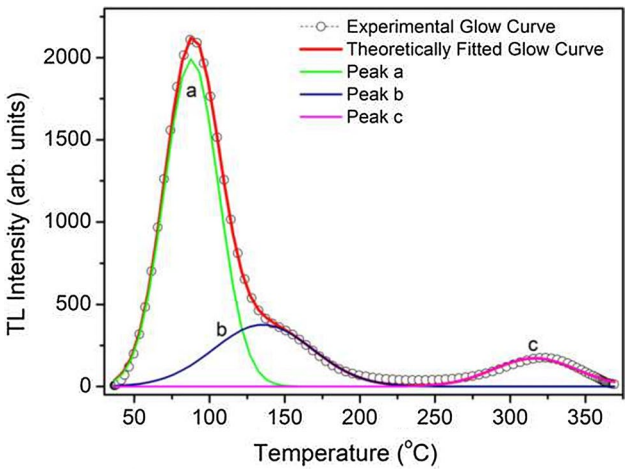


**Fig. 19** Comparison between the experimental (–o–) and the theoretically (—) fitted TL glow curves of $SrB_4O_7$:$Eu^{3+}$ (0.2 mol%) microphosphor (annealed at 700 °C for 2 h) exposed to 1.0 kGy dose of γ -rays from $Co^{60}$ source. Deconvoluted single fitted glow curves, a, b and c (—) are also shown

boron, oxygen, and europium with the appropriate amount of concentration. The Photoluminescence study of $SrB_4O_7$:$Eu^{3+}$ (0.2 mol%) microcrystalline phosphor annealed and quenched at 700 °C for 2 h shows the excitation peaks (recorded at 420 nm and 615 nm emissions) in the range 200–600 nm. It shows two visible shoulders at ~ 300 nm and 358 nm with corresponding to f-d transitions ($4f^6 5d$—$4f^7$) ($^8S_{7/2}$) of these transitions are arises from divalent europium ion in the host lattices. The PL emission spectra shows a blue emission band with ~ 310 nm and ~ 420 nm peaks which can be attributed for $Eu^{2+}$ (4f 5d) transitions. The series of emission peaks between 500 and 770 nm which corresponds to $^5D_0$—$^7F_J$ (J = 0, 1, 2, 3, and 4) transition of $Eu^{3+}$ ions under excitation with wavelengths 250, 260, 280 and 395 nm. The $SrB_4O_7$:$Eu^{3+}$ microphosphor was irradiated for different doses of gamma rays from $^{60}$Co source. The TL intensity found to be maximum for the 0.2 mol% doping of europium for the sample which was annealed and quenched at 700 °C for 2 h. The exact peak positions and the number of peaks in TL glow curve were confirmed by $T_m$-$T_{stop}$ method. The three peaks were revealed at positions 88, 138 and 318 °C. The TL glow curve was deconvoluted by the Computerized Glow Curve Deconvolution (CGCD) method and trapping parameters were calculated. All the three peaks were found to follow general order of kinetics. The dosimetry characteristics, such as, high sensitivity (comparable to TLD-900 and LiF TLD-700H), low fading (around 5% fading that of 318 °C peak), wide dose response (commercially available phosphors saturate around 100 Gy while the newly developed $SrB_4O_7$:$Eu^{3+}$ microphosphor does not saturate up to 10 kGy). All these properties make it a good candidate for TL dosimetry of high-energy radiations (Figs. 18, 19).

**Acknowledgements** One of the authors would like to thank the Inter-University Accelerator Centre (IUAC) for financial assistance under the UFUP project (File # UFR-64325).

## References

1. Bøtter-Jensen L, Larsen NA, Markey BG, McKeever SWS (1977) $Al_2O_3$: C as a sensitive OSL dosemeter for rapid assessment of environmental photon dose rates. Radiat Meas 27:295–298
2. Kortov V (2007) Materials for thermoluminescent dosimetry: Current status and future trends. Radiat Meas 42:576–581
3. McKeever SWS, Moscovitch M, Townsend PD (1995) Thermoluminescence dosimetry materials: properties and uses. Nuclear Technology Publishing, Ashford, UK
4. McKeever SWS (1985) Thermoluminescence of Solids. Cambridge University Press, Cambridge Solid State Science Series
5. Akella A, Keszler DA (1995) Structure and $Eu^{2+}$ luminescence of dibarium magnesium orthoborate. Mater Res Bull 30:105–111
6. Machida K, Adachi G, Shiokawa J, Shimada M, Koizumi M (1980) Luminescence of high-pressure phases of $Eu^{2+}$-activated $SrB_2O_4$. J Lumin 21:233–237
7. Furetta C, Kitis G, Weng PS, Chu TC (1999) Thermoluminescence characteristics of $MgB_4O_7$: Dy, Na. Nucl Inst Methods in Physics Research A 420:441–445
8. Fukuda Y, Mizuguchi K, Takeuchi N (1986) Thermoluminescence in sintered $CaB_4O_7$: Dy and $CaB_4O_7$:Eu. Radiat Prot Dosim 17:397–401
9. Karali T, Townsend PD, Prokic M, Rowlands AP (1999) Comparison of TL spectra of co-doped dosimetric materials. Rad Prot Dos 84:281–284

10. Bajaj NS, Omanwar SK (2013) Thermoluminescence study of $SrB_4O_7$: Cu phosphor prepared by combustion synthesis. Int J Modern Phys Conf Series 22:404–407
11. Li J, Hao JQ, Li CY, Zhang CX, Tang Q, Zhang YL, Su Q, Wang SB, (2005) Thermally stimulated luminescence studies for dysprosium doped strontium tetraborate. Radiat Meas 39:229–233
12. Gou J, Wang Y, Jiao H (2009) Luminescence and energy transfer of Eu- and Gd-Coactivated $SrB_4O_7$ as a potential tunable phosphor. Electrochem Solid-State Lett 12:J87–J91
13. Gao Y, Shi C, Wu Y (1996) Luminescence properties of $SrB_4O_7$: Eu, Tb phosphors. Mater Res Bull 31:439–444
14. Mikhail P, Hulliger J, Schnieper M, Bill H (2000) $SrB_4O_7$: $Sm^{2+}$ crystal chemistry, Czochralski growth and optical hole burning. J Mater Chem 10:987–991
15. Schipper WJ, Van der Voort D, van den Berg P, Vroon ZAEP, Blasse G (1933) The luminescence of europium in strontium borates. Mater Chem Phys 33:311–317
16. Atuchin VV, Kesler VG, Zaitsev AI, Molokeev MS, Aleksandrovsky AS, Kuzubov AA, Ignatova NY (2013) Electronic structure of α-$SrB_4O_7$: experiment and theory. J Phys Condens Matter 25:085503
17. Wang L, Wang Y, Wang D, Zhang J (2008) Electronic structure calculations of $SrB_4O_7$ and $SrB_4O_7$: Eu crystals. Solid State Commun 148:331–335
18. Oseledchik YU, Prosvirnin AL, Starshenko VV, Osadchuk VV, Pisarevsky AI, Belokrys SP, Korol AS, Svitanko NV, Selevich AF, Krikunov SA (1994) Crystal growth and properties of strontium tetraborate. J Cryst Growth 135:373–376
19. Shionoya S, Yen WM (1999) Phosphor Handbook. CRC Press, Washington DC, Boca Raton, pp 391–432
20. Zhiwu P, Qiang S (1993) The valence change from $RE^{3+}$to $RE^{2+}$ (RE = Eu, Sm, Yb) in $SrB_4O_7$: RE prepared in air and the spectral properties of $RE^{2+}$. J Alloy Compd 198:51–53
21. Schipper WJ, Meijerink A, Blasse G (1994) The luminescence of $Tm^{2+}$ in strontium tetraborate. J Lumin 62:55–59
22. Lacam A, Chateau C (1989) Highpressure measurements at moderate temperatures in a diamond anvil cell with a new optical sensor: $SrB_4O_7$:$Sm^{2+}$. J Appl Phys 66:366–372
23. Stefani R, Maia A, Kodaira CA, Teotonio E, Felinto M, Brito HF (2007) Highly enhanced luminescence of $SrB_4O_7$:$Eu^{2+}$ phosphor prepared by the combustion method using glycine as fuel. Opt Mater 29:1852–1855
24. Pan F, Shen G, Wang R, Wang X, Shen D (2002) Growth, characterization and nonlinear optical properties of $SrB_4O_7$ crystals. J Cryst Growth 241:108–114
25. Inaba S, Machida T, Asakawa H, Komatsu R (2017) Effects of temperature gradient on growth of $SrB_4O_7$ crystals by the micro-pulling-down method. Trans Mat Res Soc Japan 42:123–126
26. Iwamoto C, Fujihara S (2009) Fabrication and optical properties of NUV-emitting $SiO_2$–$SrB_4O_7$:$Eu^{2+}$ glass–ceramic thin films. Opt Mater 31:1614–1619
27. Kadam RM, Rajeswari B, Mohapatra M, Porwal NK, Hon NS, Seshagiri TK, Natarajan V (2015) Radiation induced centers in irradiated $SrB_4O_7$ doped europium and their role in thermally stimulated reactions: Thermally stimulated luminescence, fluorescence and electron paramagnetic resonance studies. J Lumin 158:475–483
28. Stefani R, Maia AD, Teotonio EES, Monteiro MAF, Felinto MCFC, Brito HF (2006) Photoluminescent behavior of $SrB_4O_7$:$RE^{2+}$ (RE = Sm and Eu) prepared by Pechini, combustion and ceramic methods. J Solid State Chem 179:1086–1092
29. Stamokostas GL, Fiete GA (2018) Mixing of $t_{2g}$ - $e_g$ orbitals in *4d* and *5d* transition metal oxides. Phys Rev B 97:085150
30. Zhong J, Chen D, Xu H, Zhao W, Sun J, Ji Z (2017) Red-emitting $CaLa_4(SiO_4)_3O$:$Eu^{3+}$ phosphor with superior thermal stability and high quantum efficiency for warm w-LEDs. J Alloy Compd 695:311–318
31. Lin CC, Tang YS, Hu SF, Liu RS (2009) $KBaPO_4$: Ln (Ln = Eu, Tb, Sm) phosphors for UV excitable white light-emitting diodes. J Lumin 129:1682–1684
32. Salah N, Sahare PD, Rupasov AA (2007) Thermoluminescence of nanocrystalline LiF:Mg, Cu. P J Lumin 124:357–364
33. Mandlik N, Dhole SD, Sahare PD, Bakare JS, Balraj A, Bhatt BC (2019) Thermoluminescence studies of $CaSO_4$: Dy nanophosphor for application in high dose measurements. App Radiat Isotop 148:253–261
34. Bakshi AK, Patwe SJ, Bhide MK, Sanyal B, Natarajan V, Tyagi AK, Kher RK (2008) Thermoluminescence, ESR and X-ray diffraction studies of $CaSO_4$: Dy phosphor subjected to post preparation high temperature thermal treatment. J Phys D Appl Phys 41:25402
35. Gaikwad J, Thomas S, Kamble S, Vidyasagar PB, Sarma A (1999) Effect of $^7$Li (45 MeV) ions on spinach leaves studied by thermoluminescence technique. Nucl Instrum Meth B 156:231–235
36. Mandlik N, Bhoraskar VN, Patil BJ, Dahiwale SS, Sahare PD, Dhole SD (2007) Thermoluminescence studies of $CaSO_4$: Eu nanophosphor for electron dosimetry. Indian J Pure Appl Phys 55:413–419
37. Bos AJJ (2007) Theory of thermoluminescence. Radiat Meas 41:S45–S56
38. McKeever SWS (1980) On the analysis of complex thermoluminescence glow-curves: resolution into individual peaks. Phys Stat Sol 62:331–340
39. Kitis G, Gomez-Ros JM, Tuyn JWN (1998) Thermoluminescence glow-curve deconvolution functions for first, second and general orders of kinetics. J Phys D: Appl Phys 31:2636–2641
40. Pagonis V, Kitis G, Furetta C (2006) Numerical and Practical Exercises in Thermoluminescence. Springer, NewYork
41. Chen R, Kirsh Y (1981) Analysis of thermally stimulated processes, 1st ed., Pergamon Press, New York 162–164
42. Chen R (1969) Glow curves with general order kinetics. J Electrochem Soc 116:1254–1257


**Publisher's Note** Springer Nature remains neutral with regard to jurisdictional claims in published maps and institutional affiliations.